Taylor & Francis
Taylor & Francis Group

European Journal of Remote Sensing

ISSN: (Print) 2279-7254 (Online) Journal homepage: https://www.tandfonline.com/loi/tejr20

Estimation of wind speed over lakes in Central Europe using spaceborne C-band SAR

Timea Katona & Annett Bartsch

To cite this article: Timea Katona & Annett Bartsch (2018) Estimation of wind speed over lakes in Central Europe using spaceborne C-band SAR, European Journal of Remote Sensing, 51:1, 921-931, DOI: 10.1080/22797254.2018.1516516

To link to this article: https://doi.org/10.1080/22797254.2018.1516516

Published online: 20 Sep 2018.

EUROPEAN JOURNAL OF REMOTE SENSING
2018, VOL. 51, NO. 1, 921–931
https://doi.org/10.1080/22797254.2018.1516516

Taylor & Francis
Taylor & Francis Group

OPEN ACCESS Check for updates

Estimation of wind speed over lakes in Central Europe using spaceborne C-band SAR

Timea Katona[a] and Annett Bartsch[b,c]

[a]Vienna University of Technology, Vienna, Austria; [b]Zentralanstalt für Meteorologie und Geodynamik, Vienna, Austria; [c]b.geos, Korneuburg, Austria

ABSTRACT

The Sentinel-1 satellite mission provides high-resolution, all-weather, day and night Synthetic Aperture Radar images. Studies about wind parameters above the ocean are frequent, inland lakes were seldom investigated. The objective of this article is to investigate the potential of C-band SAR for wind retrieval over lakes for evaluation of representativeness of meteorological station data. A number of lakes from Austria and Hungary (lakes in Salzkammergut, Lake Neusiedl and Lake Balaton), where wind measurements from automatic weather stations are available from the surroundings, has been selected for this study. Functions for speed retrieval are developed from empirical relationships for both available polarizations, VV and VH. Meteorological station data are used for calibration and validation. Best results were obtained for VV although with a dependency on incidence angle. Functions for different incidence angles according to the wind speed were, therefore, determined. There is a good correlation between the measured and the calculated wind speed (R of 0.71–0.91 for calibration sites; average R 0.71 for all sites). Average wind speed patterns for the lakes can be derived, but need to be analyzed separately for descending and ascending acquisitions due to difference in daytime (morning versus late afternoon).

ARTICLE HISTORY
Received 16 March 2018
Revised 20 August 2018
Accepted 22 August 2018

KEYWORDS
Radar; Sentinel-1; lakes; Austria; Hungary

The vast majority of in situ wind speed measurements comes from stations on land area. Such data are, however, also required over water surfaces for a range of applications including shipping, weather forecasting and the energy sector. Microwave satellite data are operationally used to derive wind speed over oceans (Hejazin, Aslebagh, & Jones, 2012; Hong & Shin, 2013; Stoffelen & Anderson., 1993; Wentz, 1992). The sensitivity of the recorded signal to wave patterns is exploited. The used scatterometers and radiometers have only very coarse spatial resolution, in the order of 25 km, but high sampling rates. This is too coarse for most inland waters. Several studies have investigated the wind speed over oceans using Synthetic Aperture Radar (SAR) due to its better spatial resolution (Alpers & Rufenach, 1979; Khandekar, Lalbeharry, & Cardone, 1994; Liu et al., 2013; Monaldo, Thompson, & Beal, 1999; Montuori, Nunziata, & Mascolo, 2012; Shen, Perrie, He, & Liu, 2014; Yang, Li, Pichel, & Li, 2011; Yang et al., 2010). SAR provides high-resolution, all-weather, day and night radar images. SAR offers much higher spatial resolution but to the expense of temporal resolution. Acquisitions are usually not available on a daily basis, even when overlapping orbits are exploited. Satellites are polar orbiting and timing is, therefore, limited to two windows, ascending pass in the evening and descending pass in the morning. An increased sampling rate can be achieved by combination of several satellites as, eg available from the Sentinel-1 mission.

The Sentinel-1A satellite has been launched on 3 April 2014. The main applications include monitoring the properties of water surfaces such as sea ice, oil spills, marine winds and also monitoring the changes over land such as agriculture, earth quakes and flood (Attema et al., 2007; Attema, Davidson, Snoeij, Rommen, & Floury, 2009). Although the Sentinel-1A satellite is a relatively new among the radar satellites, it is already used by several studies to investigate the wind parameters over larger water surfaces (La, Khenchaf, Comblet, & Nahum, 2016a, 2016b, 2016c). ESA (European Space Agency) provides a level 2 wind product for ocean areas (Level-2 Ocean (OCN) product) using wind direction data from ECMWF products (ESA, 2013). Inland lakes are not covered and have not been investigated in detail so far. The sensitiveness of C-band SAR to waves and, thus, wind action may be of support for assessment of representativeness of meteorological stations for lakes in their proximity and complement such measurements.

The Sentinel-1A satellite uses C-band (5.3 GHz) SAR for sensing, which is of advantage for the investigation of the wind speed and backscatter relation over the water surfaces. Rain may also have influence on water surface backscatter (Ku-band) especially at

CONTACT Timea Katona timea.katona@tuwien.ac.at Vienna University of Technology, Vienna, Austria

lower wind speed (Contreras, Plant, Keller, Hayes, & Nystuen, 2003). However, the two-way attenuation is negligible for C-band compared to Ku-band (Sullivan, 2000, p. 84).

High precision wind speed retrieval from active microwave satellites depends also on the capability to obtain measurements at multiple incidence angles at the same time. This is considered in the design of scatterometer, but not available from SAR. The wind speed accuracy is, therefore, lower, although the high spatial detail can be gained.

The objective of this study is to evaluate the potential of C-band SAR, specifically Sentinel-1, for wind speed patterns over lakes. The aim is first to evaluate the representativity of meteorological stations installed along the shorelines for the lakes and second to obtain typical patterns of wind speed on the lakes. The accuracy is quantified. A subset of lakes from Austria and Hungary, where wind measurements from automatic weather stations are available, has been selected. Functions for speed retrieval are developed from empirical relationships. Meteorological station data are used for calibration as well as validation.

Study areas

Five lakes have been investigated for this study: the Lake Neusiedl (320 km^2 – without reed belt 140 km^2, 115 m a.s.l.), Traunsee (24.4 km^2, 423 m a.s.l.), Attersee (46.2 km^2, 469 m a.s.l.) and Mondsee (13.8 km^2, 481 m a.s.l.) in Austria and the Balaton (600 km^2, 105 m a.s.l.) in Hungary. Meteorological data from the national weather services (ZAMG in Austia and OMSZ in Hungary) are available for each lake for at least one station. This includes Podersorf and Neusiedl am See (Lake Neusiedl), Altmünster and Gmunden (Traunsee), Vöcklabruck (Attersee), Mondsee (Mondsee) and Siófok (Balaton) (Figure 1).

The lakes were divided into groups representing three distinct regions: Mondsee, Traunsee and Attersee constitute the group of lakes of the mountainous Salzkammergut. They are comparably deep and have been formed during former glaciations (Behbehani et al., 1987; Nauwerck, 1991; Schneider, Müller, & Sturm, 1987). They are surrounded by mountains up to 2100 m high. Lake Neusiedl and Lake Balaton are much larger and are only surrounded by moderate hills exceeding the lake by 438 m. They are shallow steppe lakes of tectonic origin. The mountains and the opened water surface determine the possible routes for wind. They are expected to vary considerably between the lakes.

Data sets

Satellite data

The orbit of Sentinel-1 is near polar and the mean deflection from the polar orbit is around 15°. Thus, in ascending case the flight direction is 345° and in descending case 195°, which means the viewing angles of the side looking system are around 75° (ascending) and 285° (descending). Sentinel-1 acquires data in C-band, approximately 5.6 cm wavelength and with different polarization combinations.

The analyses period for the study is between 1st of October 2014 and 30rd of September 2015. Therefore, only the recordings of the Sentinel-1A were considered. The repeat cycle of the Sentinel-1A is 12 days. However, in some cases the image shave not been acquired. Sentinel data can be freely downloaded from the website of the ESA Scientific Data Hub (https://scihub.copernicus.eu/dhus/#/home). The name of the downloaded folder contains the main information of the product. Furthermore, the recording date, Absolut Orbit Number, Mission Data Take ID and the Product Unique ID.

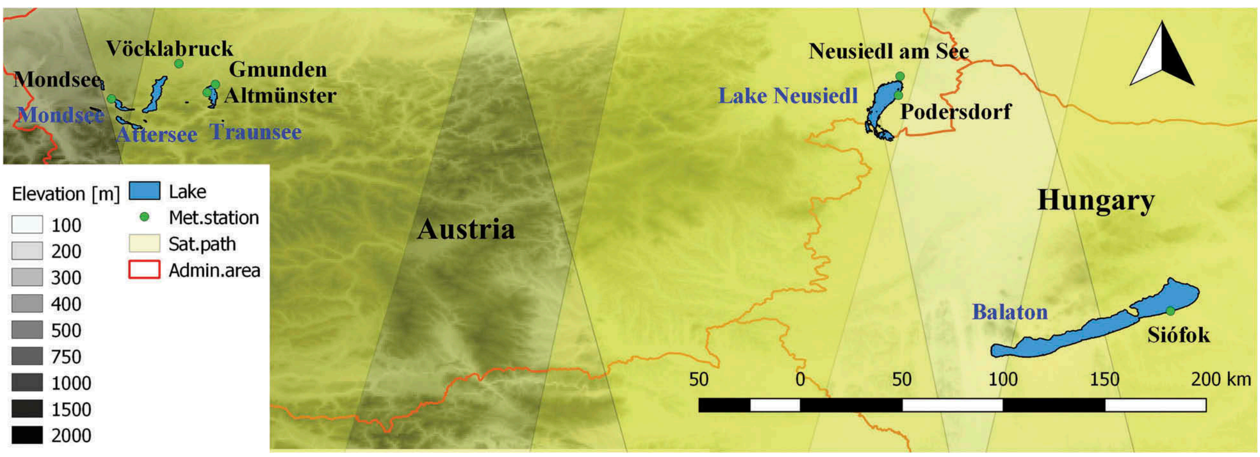

Figure 1. Location of the investigated lakes (extents derived from Sentinel-1), meteorological stations (ZAMG and OMSZ), country borders, terrain (source: http://www.diva-gis.org/gdata) and Sentinel-1A paths relevant for the groups of investigated lakes (source: ESA Sentinel scientific data hub, yellow shades indicate degree of overlap).

Only images in interferrometric wide (IW) swath mode have been considered for this study. The used nominal resolution is 10 m. The swath width is 250 km and data over Central Europe are taken at VV and VH polarization. The GRD (Ground Range Detected) processing level has been used, since only backscatter intensity values are considered for this study.

The image acquisition geometry types can be classified in seven groups. In two groups (an ascending and descending) the whole Lake Neusiedl is contained. These two groups and one more descending cover the Balaton, and one more ascending group the half of the Balaton with Siófok. The lakes of Salzkammergut are included in one descending group. In two of the groups (an ascending and descending) part of the lakes of Salzkammergut and half of Lake Neusiedl are covered. However, if a lake falls exactly between two adjacent images and therefore only a quarter of the lake is captured, the image was rejected.

In total 165 acquisitions have been used for this study. Descending images are usually acquired between 4:53 and 5:17 UTC in the morning and ascending at 16:33–16:50 UTC in the afternoon.

For quality control EOSDIS was used. This database provides satellite images taken from various NASA devices (Esfandiari, Ramapriyan, Behnke, & Sofinowski, 2006).

The digital elevation model of the Shuttle Radar Topographic Mission (SRTM) (Farr et al., 2007) has been utilized for terrain correction. The SRTM 3 arc second version – approximately 90-meter resolution – has been chosen.

Meteorological data

The meteorological dataset contains 10-min average wind speed and wind direction, maximum wind speed and its direction and time within the 10 min recorded in the stations Mondsee, Vöcklabruck, Altmünster, Gmunden, Neusiedl am See and Podersdorf. In the case of latter two also air temperature and surface temperature are measured by the Austrian Central Institution for Meteorology and Geodynamics (ZAMG). The Hungarian Meteorological Service (OMSZ) provided the 10-min average wind speed and wind direction data recorded in the station Siófok and the water temperature measurements are available from the Middle Transdanubian Water Directorate (KDTVIZIG) Balaton Water Management Branch recorded daily at the station Siófok near to the surface at 7 am. In the case of Balaton and lakes of Salzkammergut the measurements, which have been granted by the meteorological services, were taken between 01.10.2014 and 31.05.2015, in the case of Lake Neusiedl for the whole period of 01.10.2014 to 30.09.2015. Wind measurements at meteorological stations are conventionally mounted at 10 m above ground.

The typical wind speed range varies between the stations. The station Altmünster has very low values and the highest measured maximal speed is only 5.2 ms^{-1} (compared to 18.0 ms^{-1} which is recorded in Podersdorf). The mean speed measured by Gmunden for all the investigated dates is also low with 1.3 ms^{-1}.

Methods

Backscatter relates to wind speed over water surfaces (Woodhouse, 2006). It increases with increasing wind speed due to the formation of capillary waves. Exponential relationships between σ_0 from co-polarized data and wind speed are reported widely in the literature (Long, Collyer, & Arnold, 1996; Rufenach, 1995; Wentz & Smith, 1999). It saturates at high wind speeds. In addition, it depends on the incidence angle and the azimuth look angle with respect to the wind direction, which conditions the periodic pattern orientation of the waves. This pattern also results in specific polarimetric properties of the return signal. The backscattered power is highest at upwind orientation (radar look direction and the wind direction aligned) and lowest at crosswind orientation of the radar beam. Models have been developed to describe these relationships (Stoffelen & Anderson, 1997). The wind direction can be obtained and considered for speed retrieval when different looking directions can be provided by the satellite. This is not applicable to SAR. An alternate source is required such as from in situ records, models or linear features (Fetterer, Gineris, & Wackerman, 1998; Gerling, 1986; Horstmann, Lehner, Koch, & Tonboe., 2000; Monaldo, Jackson, Li, & Pichel, 2015; Vachon & Dobson, 1996; Wackerman, Rufenach, Schuchman, Johannessen, & Davidson, 1996). Koch (2004) suggests the so-called local gradient method, which results in lower spatial resolution in the order of 1 x 1 km. This is not considered applicable for the studied lakes which have a width of mostly less than 5 km. The issue of lacking wind direction is addressed using in situ measurements for this study. Zhang and Perrie. (2012) as well as Huang, Liu, Li, Zhang, and Yu (2017) suggested the use of cross-polarized information (VH) for retrieval for wind speeds up to 25 ms^{-1} with a linear equation. This has been validated for wind speed at a height of 10 m. The relationship of VH with σ_0 has been shown to be independent from incidence angle. Nevertheless, both VV and VH acquisitions have been considered for this study.

All images were visually inspected in a first step in order to exclude occasions with ice cover. The selection process was supported by water temperature measurements and optical satellite data from

EOSDIS. Due to the fact that EOSDIS provides optical images, lakes are obscured during cloudy weather.

All SAR images have been conventionally pre-processed including radiometric calibration, speckle filtering (Lee Sigma Filter, 7 × 7 window size), range doppler terrain correction (based on SRTM digital elevation model) and eventually σ_0 converted from linear to db units. Terrain correction is necessary for correction of the offset of the lakes as they are located up to 481 m a.s.l. (see section 1). Data have been subset over the lakes of interest.

Scenes with calm wind conditions have been used to derive lake masks. The typical low backscatter allows a straight forward separation of water surfaces from the surrounding terrain in case of C-band (Bartsch, Pathe, Wagner, & Scipal, 2008).

In a further step, an empirical relationship is determined between backscatter and wind speed for specific incidence angles. The in situ datasets have been split up into a calibration and validation record. Since these values are only valid near the stations, only the initial empirical model is applied for all lake surfaces and dates in order to obtain typical wind speed patterns.

The station Neusiedl am See was not taken into account for calibration, because it is not located directly at the shore of Lake Neusiedl. The Station Podersdorf and also Siófok are located within a few meters from the water surface. Also Mondsee, Altmünster and Gmunden have similar position as Neusiedl am See. The measured velocities taken by the Station Vöcklabruck were not taken into account even for the validation. The station Vöcklabruck is in huge distance from Attersee, not mentioned the fall between the lake and the station. The Mondsee station was also considered for validation only due to its location.

Transects perpendicular to the shoreline have been used to select backscatter samples from the lake surfaces. The starting point is in all cases the coordinate of a meteorological station. The distances between the sampling points are always equal and larger than the pixel size. The corresponding 10 min average wind speed has been selected from the in situ records. Only VV-polarized images were eventually considered due to its better relationship than VH with wind speed at 10-m height. Figure 2 demonstrates this issue for an example on Lake Balaton.

In a second quality control step, scatterplots for the calibration records have been derived and visually inspected. If a single point deviated from the adjacent points the satellite image was investigated again. Not only ice can affect backscatter but a bigger ship can also cause high backscatter. If the satellite image indicated the presence of a boat the backscatter value of that point was rejected.

Linear, polynomial and exponential curves were tested. The exponential fitting had the lowest errors

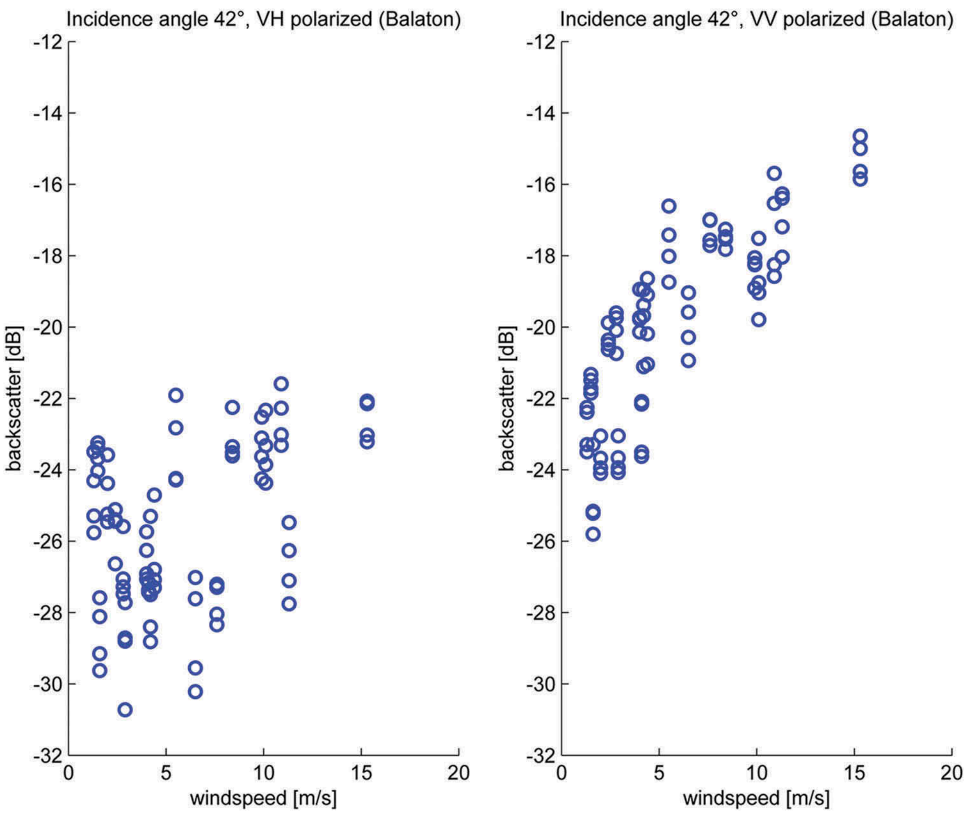

Figure 2. Backscatter with wind speed comparison at VH-polarization (left panel) and VV-polarization (right panel). Lake Balaton, Sz´antod-Tihany transects.

in most of the cases which means the exponential fit is better to use to get the velocity v based on the backscatter (σ).

The empirical formula for calculating the wind speed is:

$$v = a \cdot \exp(b \cdot \sigma) \quad (1)$$

A second fitting step considered the derived wind speed with respect to the incidence angle. Again the best fitted curve was exponential; however, in this case only polynomial and exponential curve were tested. The calculated function gives the coefficients a and b. For the evaluation and validation these coefficients were used for the exponential function. Specified with the parameters the velocity was (separately for ascending and descending orbit) calculated as:

$$v = f(\sigma, \Theta) = a(\Theta) \cdot \exp(b(\Theta) \cdot \sigma) \quad (2)$$

where, a and b are the empirical coefficients, σ is the backscatter and θ is the incidence angle. The backscatter depends on the incidence angle; however, hence in the case of (2) the empirical coefficients depend on the incidence angle.

Wind speed is highly variable in horizontal distance. Averages over selected areas are, therefore, chosen for evaluation of the derived wind speed maps. In order to obtain a backscatter sample for validation, square areas on the lakes next to the stations of 10 × 10 m size have been defined. The distances from the stations are varying according to the distance between the station and the water surface and the shape of the coast. The distances are the following, 180 m to the West from Siófok, 170 m to Southeast from Mondsee, 296 m to Southwest from Gmunden, 620 m to the East from Altmünster, 360 m to the West from Podersdorf, 2826 m to the South from Neusiedl am See and in one group only the half of the lake is covered where the incidence angle is 30° the distance of the polygon is 4377 m from Podersdorf and 8720 m from Neusiedl am See. For validation the Pearson correlation and root mean square error has been used.

The validation was carried out for the groups with the incidence angle between 30° and 42°. For the correlation all the velocity measurements of the meteorological stations (except Vöcklabruck) and the calculated mean wind speed of the data contained by the nearest validation area to the certain station were taken (Table 1). Previous investigations of C-band SAR over oceans also evaluated results by comparison to scatterometer measurements (Yang et al., 2011, 2010). C-band scatterometer data gridded to 12.5 km were used for the cross-comparison. This grid size is, however, too coarse for the lakes of this study and this assessment method, therefore, not applicable.

The resulting wind speed maps have been averaged separately for descending and ascending to obtain information on typical wind speed patterns in the morning and late afternoon.

Results

The wind speed range which is available for the determination of the empirical relationship varies between ascending and descending, evening and morning measurements, respectively. Higher wind speeds are observed in the evening. Examples of backscatter statistics for different wind speed ranges from Lake Balaton and Lake Neusiedl are shown in Figure 3. This difference results in better fit of the functions to the calibration data and correlation with the validation data in ascending images (Table 1). The average correlation is higher (0.7 versus 0.65) and the RMSE lower. The latter applies especially to the larger lakes Neusiedl and Balaton which have more frequent high wind speeds. This results also in differences between the derived empirical relationships from ascending and descending orbits respectively (Figure 4).

Table 1. Data availability, properties from Sentinel-1 and meteorological station data. * lower number of measurements at meteorological station than in others of the same group. Validation results: RMSE in ms^{-1} and R^2. Calibration based on single pixel values from transects, validation on averages of polygons. Num. – Number of images; Inc. – Incidence angle; Dist. – Distance between meteorological station and lake.

								Used for	
	Lake	Num.	Inc. [°]	Met. Station	Dist. [m]	RMSE	R^2	Calc.	Valid.
Ascending	Balaton	15	32	Siófok	22.1	2.6760	0.8159	x	x
	Traunsee	19	33	Gmunden	426	1.3723	0.6360		x
		*14		Altmünster	208	0.9099	0.0716		x
	Neusiedl	18	37	Podersdorf	16.2	2.2397	0.8371	x	x
	(T_w-Rust)			Neusiedl am See	2360	1.4982	0.6317		x
	Balaton	12	42	Siófok	22.1	2.5528	0.8537	x	x
Descending	Neusiedl	19	30	Podersdorf	16.2	2.2870	0.7352	x	x
	(T_w-Rust)			Neusiedl am See	2360	1.5201	0.7308		x
	Balaton	13	33	Siófok	22.1	1.3893	0.7421	x	x
	Mondsee and Traunsee	14	35	Gmunden	426	1.2201	0.7317		x
		*11		Altmünster	208	2.5813	0.5772		x
		*13	37	Mondsee	94.9	0.9894	0.8106		x
	Neusiedl	22	40	Podersdorf	16.2	1.1222	0.9047	x	x
	(T_w-Rust)			Neusiedl am See	2360	2.1545	0.6862		x
	Balaton	13	42	Siófok	22.1	1.5326	0.9147	x	x

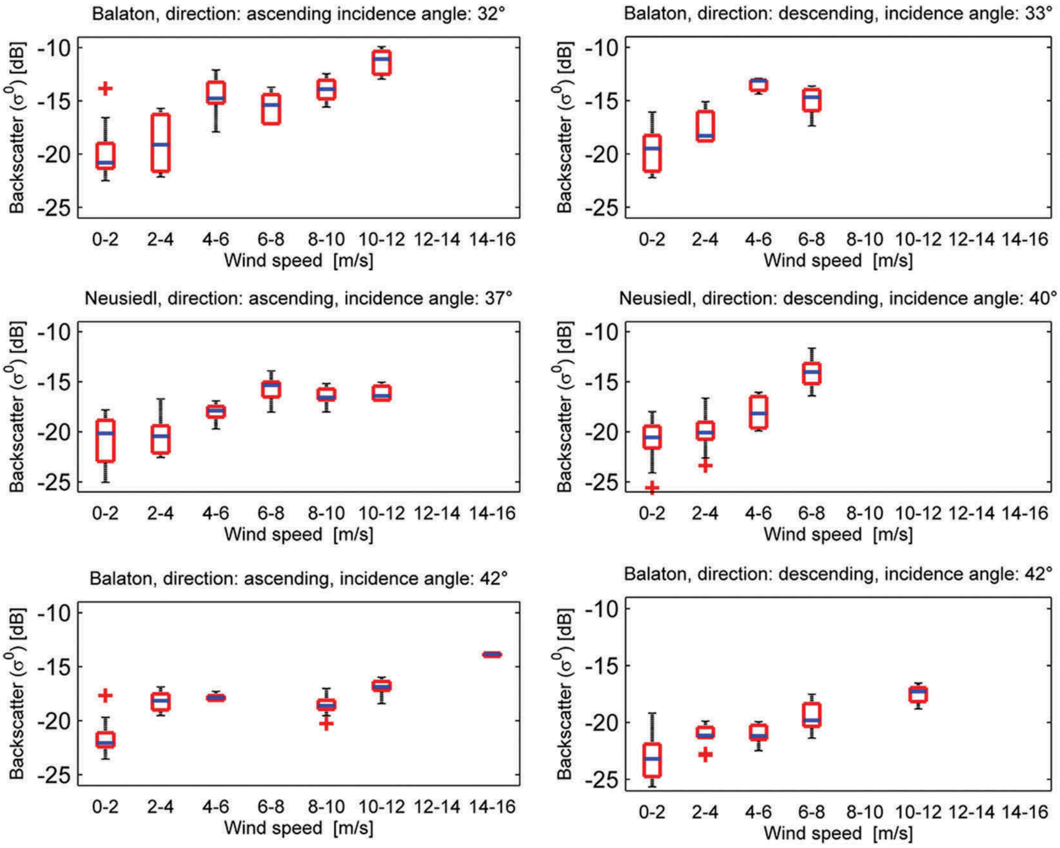

Figure 3. Examples of backscatter statistics (box plots) for different wind speed ranges from Lake Balaton and Lake Neusiedl.

The number of available acquisitions varied between the lakes and stations (Table 1). 145 Wind maps could be derived, 53 for Balaton, 59 for Lake Neusiedl and 33 for the lakes of Salzkammergut.

The prevailing wind direction and the role of the relief are observable in the final maps (Figures. 5–7). The NW to SE oriented striping patterns in the Lake Balaton and Lake Neusiedl indicate NW winds. This can be confirmed with wind direction measurements available from station data (Figure 8). The differences between morning and evening are largest for Lake Balaton, they are in the order of 3 dB. The lowest wind speeds and day time difference have the Salzkammergut lakes. They show, however, the highest range in wind speeds during the morning acquisitions. Parts of the lakes have very calm surfaces with on average less than 1 ms^{-1} wind

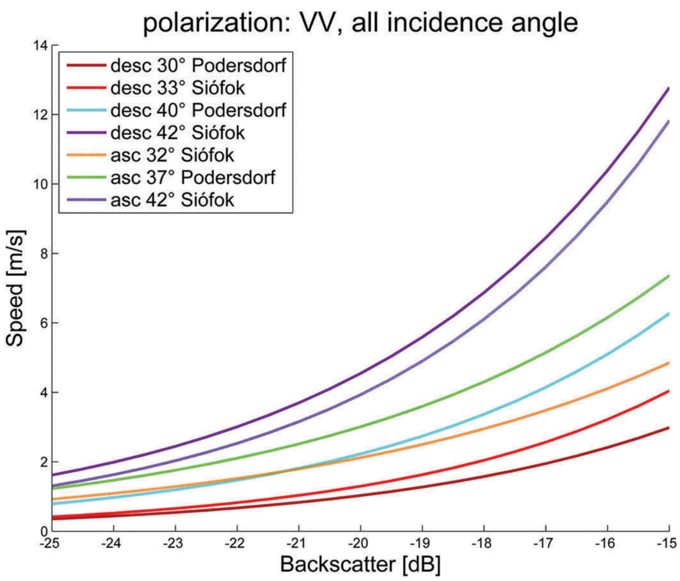

Figure 4. Empirically derived functions for two calibration sites representing six incidence angle groups (30, 32, 33, 37, 40 and 42?) and VV polarization. Descending (morning, lower wind speeds in calibration sample) cases are indicated by dashed lines, ascending (evening, higher wind speeds in calibration sample) cases by solid lines.

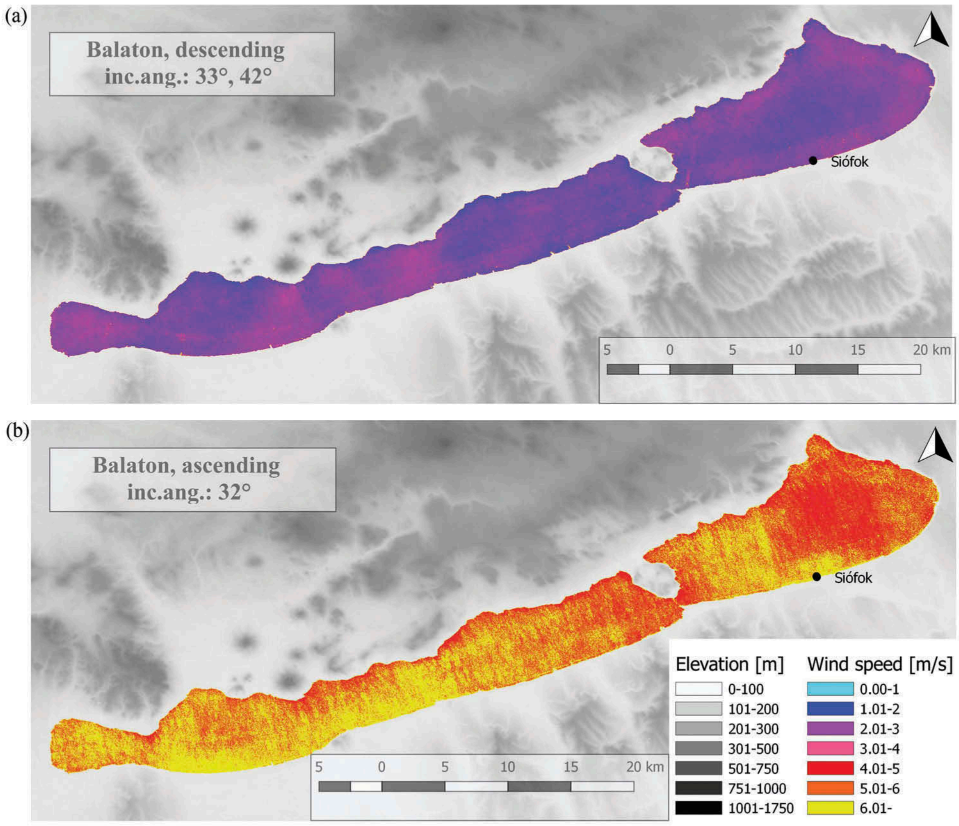

Figure 5. Lake Balaton: Average wind speed during the observation period for morning (descending) and evening (ascending) Sentinel-1A acquisitions.

speed. This applies to western parts of Attersee and Mondsee. The Mondsee meteorological station is located near such a zone.

The variation of wind speed across the lakes differs between morning and evening for same lakes. Values are higher in the northern than in the southern part in the morning for Lake Neusiedl. This pattern is reversed in the evening. Both meteorological stations represent the northern part. The centre of the eastern part of Lake Balaton is calmer than the surroundings in the morning. This changes also in the ascending acquisitions.

The patterns on Traunsee are similar in morning and in the evening except in the most southern tip. The western side where Altmünster station is located, average wind speed remains below 2 ms^{-1} in both cases. The results near the Gmunden station on the opposite side of the lake show average values of 2–3 ms^{-1}.

Discussion

Results confirm that exponential functions can be applied to derive wind speed from co-polarized measurements at C-band. The in the literature proposed linear retrieval (Zhang & Perrie., 2012) from cross-polarized data could not be verified for the standard 10 m height wind measurements of terrestrial meteorological stations. The maximum of observed wind speeds has been in the order of 16 ms^{-1}, much lower than the investigated range by Zhang and Perrie. (2012, 25 ms^{-1}). For comparison with results from oceanographic applications, a conversion to 10 m height over water would be necessary, as this is the used standard height in such cases (Stull, 2012). Our analyses includes the assessment of representativeness of meteorological stations over land. It also has to be noted that the satellite images taken on descending and ascending path show differences. The satellite images which are taken during the descending path show higher backscatter ratio below incidence angles of 42° (at 42° in ascending case, the measured velocities are extreme high). This can be due to the prevailing wind direction which is closer to the looking direction of the satellite. The measured velocities are much higher at ascending acquisitions which results in a different distribution of the samples and eventually the fitted empirical function.

The correlation between the measured and the calculated wind speed shows good correlation. In some cases lower correlation is caused by the higher distance between the station and the water body (Table 1). The RMSE indicates better correlation for Traunsee for the case when the images are taken on ascending path.

The prevailing wind direction at Podersdorf corresponds to crosswind (ascending) to downwind

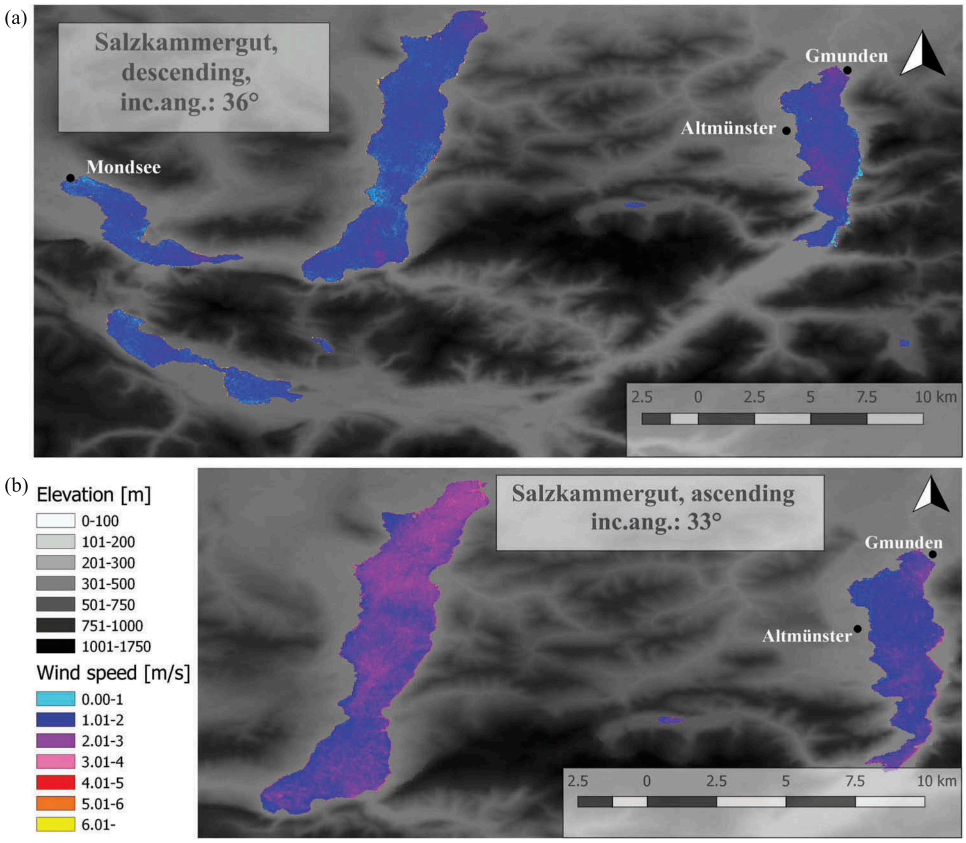

Figure 6. Salzkammergut: Average wind speed during the observation period for morning (descending) and evening (ascending) Sentinel-1A acquisitions.

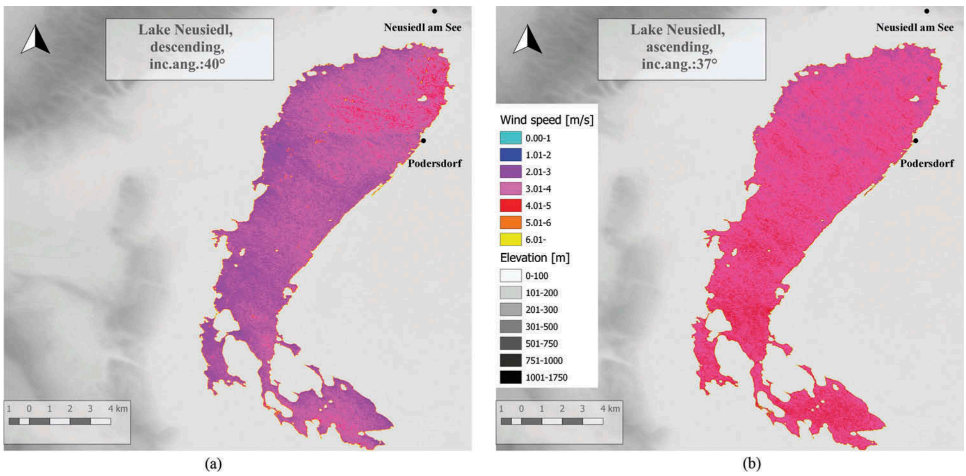

Figure 7. Lake Neusiedl: Average wind speed during the observation period for morning (descending) and evening (ascending) Sentinel-1A acquisitions.

(descending) observations from space. This is similar for Siófok. Both locations show comparably high RMSE which might be related to the lacking correction for wind direction. The Pearson correlation is on the contrary comparably high in both cases as the wind direction is similar between the acquisitions. Deviations due to the asymmetry of the waves do, therefore, not change considerably from acquisition to acquisition.

Wind direction patterns are more diverse at the Salzkammergut lakes what adds to the issue that stations are not located directly at the lakes. Pearson correlations are lowest. RMSE is between 1 and 2 ms^{-1} but numbers are in general smaller.

The velocity of the wind is not a constant value, the wind speed and its direction can change rapidly that is why the 10-min mean values measured (and averaged) by the meteorological

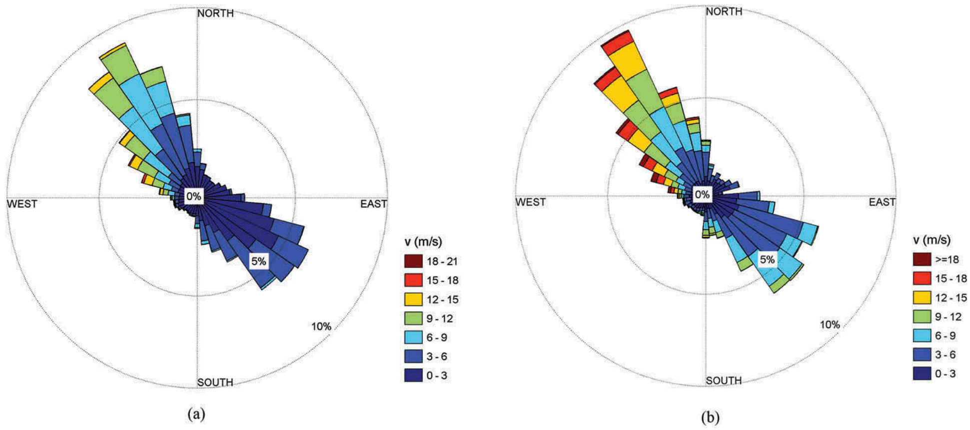

Figure 8. Prevailing wind direction measured at the Podersdorf Meteorological Station. Left: direction of the wind spikes Right: direction of the 10-min average (Data source: ZAMG).

stations cannot be taken as a strict value (variance around the mean wind speed occurs) and for accurate coefficients and functions the wind speed measuring at the certain moment would be necessary. Since the permanent recording would be unwanted because of the storage of the huge amount of data, the synchronization of the meteorological station and satellite (saving the actual measurement at the time when the satellite passes the station) would be beneficial.

The availability of Sentinel-1 B since 28 April 2016 increases data availability, but images are acquired at similar day times and looking directions.

Models used for operational retrieval over oceans like CMOD5 (Hersbach, Stoffelen, & De Haan, 2007) utilize different incidence angles, as available from scatterometer, to account for dependence on direction, which is not possible in case of SAR. The wind direction, therefore, has an impact on the RMSE of the determined wind speed, but is in the presented case limited for correlations and, thus, the variations reflected in the time series. This can be attributed to the prevailing wind directions at the analyzed lakes.

Spatial patterns of wind speed suggest that the currently available stations at the Austrian lakes are only representative for a proportion of the lakes. The retrievals from Sentinel-1 at VV polarization can help to identify these patterns, although multi-incidence angle capability is lacking. Lower correlations and thus lower representativeness of the stations for water applications can be observed for stations located away from the shores. SAR records may be used to quantify the impact.

The availability of morning and evening acquisition in irregular intervals limits the application potential of SAR derived wind speed information. General patterns can be, however, derived and used for evaluation of in situ observations near the lakes and model results which are based on them.

Acknowledgments

Meteorological station data have been provided by the Austrian Central Institution for Meteorology and Geodynamics (ZAMG) for stations in Austria. The Hungarian Meteorological Service (OMSZ) provided the 10-min average wind speed and wind direction data recorded for Hungarian stations.

Disclosure statement

No potential conflict of interest was reported by the authors.

References

Alpers, W., & Rufenach, C. (1979, Sep). The effect of orbital motions on synthetic aperture radar imagery of ocean waves. *IEEE Transactions on Antennas and Propagation*, *27*(5), 685–690.

Attema, E., Bargellini, P., Edwards, P., Levrini, G., Lokas, S., Moeller, L., Rosich-Tell, B.,Secchi, P., Torres, R., Davidson, M. & Snoeij, P., (2007). Sentinel-1-the radar mission for GMES operational land and sea services. *ESA Bulletin*, *131*, 10–17.

Attema, E., Davidson, M., Snoeij, P., Rommen, B., & Floury, N., "Sentinel-1 mission overview," *2009 IEEE International Geoscience and Remote Sensing Symposium*, Cape Town, 2009, pp. I–36. doi: 10.1109/IGARSS.2009.5416921

Bartsch, A., Pathe, C., Wagner, W., & Scipal, K. (2008). Detection of permanent open water surfaces in central Siberia with ENVISAT ASAR wide swath data with special emphasis on the estimation of methane fluxes from tundra wetlands. *Hydrology Research*, *39*(2), 89–100.

Behbehani, A.-R., Müller, J., Schmidt, R., Schneider, J., Schröder, H., Strackenbrock, I., & Sturm, M. (1987). *Sediments and sedimentary history of Lake Attersee (Salzkammergut, Austria)* (pp. 233–246). Dordrecht: Springer Netherlands.

Contreras, R.F., Plant, W.J., Keller, W.C., Hayes, K., & Nystuen, J. (2003). Effects of rain on Ku-band backscatter from the ocean. *Journal of Geophysical Research*, *108*, 3165. . C5

ESA. 2013. "Sentinel-1 Product Specification." Ref: S1-RS-MDA-52-7441.

Esfandiari, M., Ramapriyan, H., Behnke, J., & Sofinowski, E., "Evolution of the Earth Observing System (EOS) Data and Information System (EOSDIS)," *2006 IEEE International Symposium on Geoscience and Remote Sensing*, Denver, CO, 2006, pp. 309–312. doi: 10.1109/IGARSS.2006.84

Farr, T.G., Rosen, P.A., Caro, E., Crippen, R., Duren, R., Hensley, S., … Seal, D. (2007). The shuttle radar topography mission. *Reviews of Geophysics*, *45*, 2.

Fetterer, F., Gineris, D., & Wackerman, C.C. (1998). Validating a scatterometer wind algorithm for ERS-1 SAR. *IEEE Transactions Geosci Remote Sensing*, *36*, 479–492.

Gerling, T.G. (1986). Structure of the surface wind field from seasaat SAR. *Journal of Geophysical Research*, *91*, 2308–2320.

Hejazin, Y., Aslebagh, S., & Jones, W.L. 2012. *Aquarius/SAC-D microlwave radiometer ocean wind speed measurements*. In 2012 Oceans. 1–4, IEEE.

Hersbach, H., Stoffelen, A., & de Haan, S. (2007). An improved C-band scatterometer ocean geophysical model function: CMOD5. *Journal of Geophysical Research: Oceans*, *112*, C3.

Hong, S., & Shin, I. (2013). Wind speed retrieval based on sea surface rough-ness measurements from spaceborne microwave radiometers. *Journal of Applied Meteorology and Climatology*, *52*(2), 507–516.

Horstmann, J., Lehner, S., Koch, W., & Tonboe., R. (2000). Computation of wind vectors over the ocean using spaceborne synthetic aperture radar. *Johns Hopkins APL Technical Digest*, *21*(1), 100–107.

Huang, L., Liu, B., Li, X., Zhang, Z., & Yu, W. (2017). Technical evaluation of Sentinel-1 IW mode cross-pol radar backscattering from the ocean surface in moderate wind condition. *Remote Sens.*, *2017*(9), 854.

Khandekar, M., Lalbeharry, L.R., & Cardone, V.J. (1994). The performance of the Canadian spectral ocean wave model (CSOWM) during the grand banks ERS-1 SAR wave spectra validation experiment. *Atmosphere-Oceans*, *32*, 31–60.

Koch, W. (2004). Directional analysis of SAR images aiming at wind direction. *IEEE Transactions Geosci Remote Sensing*, *42*, 702–710.

La, T.V., Khenchaf, A., Comblet, F., & Nahum, C., "Study of sensitivity in wind direction retrieval from Sentinel-1 images," *2016 2nd International Conference on Advanced Technologies for Signal and Image Processing (ATSIP)*, Monastir, 2016a, pp. 581–585. (a). doi: 10.1109/ATSIP.2016.7523148

La, T.V., Khenchaf, A., Comblet, F., & Nahum, C., "Assessment of inversion models for sea surface wind speed retrieval from Sentinel-1 data," *2016 2nd International Conference on Advanced Technologies for Signal and Image Processing (ATSIP)*, Monastir, 2016b, pp. 577–580. (b). doi: 10.1109/ATSIP.2016.7523147

La, T.V., Khenchaf, A., Comblet, F., & Nahum, C., "Study of wind speed retrievals from Sentinel-1 images using physical models," *2016 10th European Conference on Antennas and Propagation (EuCAP)*, Davos, 2016c, pp. 1–4. (c). doi: 10.1109/EuCAP.2016.7481445

Liu, G., Yang, X., Li, X., Zhang, B., Pichel, W., Li, Z., & Zhou, X. (2013). A systematic comparison of the effect of polarization ratio models on sea surface wind retrieval from C-band synthetic aperture radar. *IEEE Journal Sel Topics Applications Earth Observ Remote Sens.* doi:10.1109/JSTARS.2013.2242848

Long, D.G., Collyer, R.S., & Arnold, D.V. (1996). Dependence of the normalized radar cross section of water waves on bragg wavelength-wind speed sensitivity. *IEEE Transactions on Geoscience and Remote Sensing*, *34*(3), 656–666.

Monaldo, F.M., Jackson, C.R., Li, X., & Pichel, W.G. (2015). Preliminary evaluation of Sentinel-1A wind speed retrievals. *IEEE Journal Sel Topics Applications Earth Observ Remote Sens.* doi:10.1109/JSTARS.2015.2504324

Monaldo, F.M., Thompson, D.R., & Beal, R.C., "Systematic comparison of RADARSAT SAR derived wind speed with buoy measurements," *Geoscience and Remote Sensing Symposium, 1999. IGARSS '99 Proceedings. IEEE 1999 International*, Hamburg, 1999, pp. 1969–1971 vol.4.

Montuori, M., Nunziata, M.F., & Mascolo, L., "Wind speed estimation in the Tyrrhenian Sea by means of X-band COSMO-SkyMed SAR data," *Advances in Radar and Remote* Sensing *(TyWRRS), 2012 Tyrrhenian Workshop on*, Naples, 2012, pp. 222–229.doi: 10.1109/TyWRRS.2012.6381133

Nauwerck, A. (1991). *The history of the genus Eubosmina in Lake Mondsee (upper Aus-tria)* (pp. 87–103). Dordrecht: Springer Netherlands.

Rufenach, C. (1995). A new relationship between radar cross-section and ocean surface wind speed using ERS-t scatterometer and buoy measurements. *International Journal of Remote Sensing*, *16*(18), 3629–3647.

Schneider, J., Müller, J., & Sturm, M. (1987). *Geology and sedimentary history of Lake Traunsee (Salzkammergut, Austria)* (pp. 227–232). Dordrecht: Springer Netherlands.

Shen, H., Perrie, W., He, Y., & Liu, G. (2014). Wind speed retrieval from VH dual-polarization RADARSAT-2 SAR images. *IEEE Transactions on Geoscience and Remote Sensing*, *52*(9), 5820–5826.

Stoffelen, A., & Anderson., D.L.T. (1993). Wind retrieval and ERS-1 scatterometer radar backscatter measurements. *Advances in Space Research*, *13*(5), 53–60.

Stoffelen, A.C.M., & Anderson, D.L.T. (1997). Scatterometer data interpretation: Derivation of the transfer function CMOD4. *Journal of Geophysical Research*, *102*, 5767–5780.

Stull, R.B. (2012). *An introduction to boundary layer meteorology* (Vol. 13). Springer Science & Business Media, Springer Netherlands.

Sullivan, R.J. (2000). *Microwave radar: Imaging and advanced concepts(Book)*. Norwood, MA: Artech House, Inc, 2000.

Vachon, P.W., & Dobson, F.W. (1996). Validation of wind vector retrieval from ERS-1 SAR images over the ocean. *Global Atmos Ocean Systems*, *5*, 177–187.

Wackerman, C.C., Rufenach, C.L., Schuchman, R., Johannessen, J.A., & Davidson, K. (1996). Wind vector retrieval using ERS-1 synthetic aperture radar imagery. *Journal of Geophysical Research*, *34*, 1343–1352.

Wentz, F.J. (1992). Measurement of oceanic wind vector using satellite microwave radiome-ters. *IEEE Transactions on Geoscience and Remote Sensing*, *30*(5), 960–972.

Wentz, F.J., & Smith, D.K. (1999). A model function for the ocean-normalized radar cross section at 14 GHz derived from NSCAT observations. *Journal of Geophysical Research: Oceans*, *104*, C5.

Woodhouse, I.H. (2006). *Introduction to microwave remote sensing*. Boca Raton: Taylor & Francis.

Yang, X., Li, X., Pichel, W.G., & Li, Z. (2011). Comparison of ocean surface winds from ENVISAT ASAR, metop ASCAT scatterometer, buoy measurements and NOGAPS model, IEEE Trans. *Geoscience Remote Sens*. doi:10.1109/TGRS.2011.2159802

Yang, X., Li, X., Zheng, Q., Gu, X., Pichel, W., & Li, Z. (2010). Comparison of ocean surface winds retrieved from quikSCAT scatterometer and Radarsat-1 SAR in offshore waters of the US West Coast. *IEEE Geoscience and Remote Sensing Letters*, *99*, 163–167.

Zhang, B., & Perrie., W. (2012). Cross-polarized synthetic aperture radar: A new potential measurement technique for hurricanes. *Bulletin Amer Meteor Social*, *93*, 531–541.